Nanoscale

PAPER

View Article Online
View Journal | View Issue

Check for updates

Cite this: *Nanoscale*, 2024, **16**, 18524

On-surface synthesis – Ullmann coupling reactions on N-heterocyclic carbene functionalized gold nanoparticles†

Nathaniel Ukah *[a,b] and Hermann A. Wegner [a,b]

Received 24th July 2024,
Accepted 3rd September 2024

DOI: 10.1039/d4nr03065f

rsc.li/nanoscale

Organic on-surface syntheses promise to be a useful method for direct integration of organic molecules onto 2-dimensional (2D) flat surfaces. In the past years, there has been an increasing understanding of the mechanistic details of reactions on surfaces, however, mostly under ultra-high vacuum on very defined surfaces. Herein, we expand the scope to gold nanoparticles (AuNps) in solution *via* an Ullmann reaction of aryl halides connected *via* N-heterocyclic carbenes (NHCs) to AuNps. Through design and syntheses of various organic precursors, we address the influence of the contact angle, reactivity of the halogen and the proximity of the entire coupling partner on on-surface reactivities, thus, establishing general parameters governing organic on-surface syntheses on AuNps in solution, in comparison with the reactivity on defined surfaces under ultra-high vacuum. The retention of such halogenated Nps even at higher reaction temperatures holds great promise in the fields of materials engineering, nanotechnology and molecular self-assembly, while expanding the toolbox of organic chemistry synthesis in accessing various covalent architectures.

Open Access Article. Published on 04 September 2024. Downloaded on 5/10/2026 11:54:49 PM.
This article is licensed under a Creative Commons Attribution 3.0 Unported Licence.

Introduction

The idea of confining reactions to a flat substrate has led to the transition of a chemical environment from a typical three-dimensional reaction space in the solution phase to a seemingly two-dimensional platform.[1–21] This new environment has the potential to facilitate alternative reaction pathways to those available in solution, giving rise to new selectivities and intermediates which are otherwise difficult to obtain *via* in-solution organic synthesis.[1–9,12,14,19] A prototype of this on-surface synthesis *via* molecule-by-molecule manipulation was reported by Ebeling and coworkers,[22] who attained a high degree of selectivity between the homo- and hetero-coupling of aryl halides by adsorbing the reaction partners to a 2D Au(111) surface followed by dehalogenation with voltage pulses. The generated radicals were dragged and dropped, using a CO-functionalized tip of an atomic force microscope (AFM), to provide organic structures which are difficult to access *via* in-solution synthesis.[22] Similarly, the group of Glorius[23] synthesized and deposited N-heterocyclic carbenes (NHCs) on crystalline gold surfaces under high vacuum and performed an Ullmann coupling of these moieties to obtain covalently linked ballbot-type repeating units of NHCs, bound to single Au ad-atoms. A combination of scanning tunnelling microscopy (STM), non-contact AFM, X-ray photoelectron spectroscopy (XPS) and density functional theory (DFT) calculations was used to determine the conformational properties, steric influence, binding mode, electronic properties, and the surface alignments of these new covalent architectures.[23] Nevertheless, these aforementioned techniques require organic precursors to be deposited under ultra-high vacuum (UHV) conditions onto highly defined single crystalline flat surfaces. Only then, visualization with AFM is possible. That way, only single molecules are produced and as such, the process is not suitable for syntheses of larger, isolatable amounts of materials. With the option to attain bulk materials in Ullmann reactions in a selective manner, we moved from defined planar surfaces under high vacuum to nanoparticles in solution, and devised a protocol for Ullmann coupling reactions using NHC-functionalized gold nanoparticles (AuNps) as a reaction platform. Our system offers advantages compared to the system of Glorius,[23] such as: (1) it avoids sublimation of molecules to the surface allowing the use of high molecular weight precursors as starting materials. This fact allows expanding the scope of on-surface reactivities to different varieties of organic materials. (2) It extends the availability of pro-

[a]*Institute of Organic Chemistry, Justus Liebig University Giessen, Heinrich-Buff-Ring 17, 35392 Giessen, Germany. E-mail: Hermann.A.Wegner@org.chemie.uni-giessen.de*
[b]*Center for Materials Research (ZfM/LaMa), Justus Liebig University Giessen, Heinrich-Buff-Ring 16, 35392 Giessen, Germany*

† Electronic supplementary information (ESI) available. See DOI: https://doi.org/10.1039/d4nr03065f

This journal is © The Royal Society of Chemistry 2024

Open Access Article. Published on 04 September 2024. Downloaded on 5/10/2026 11:54:49 PM.
This article is licensed under a Creative Commons Attribution 3.0 Unported Licence.

ducts from single molecules to larger amounts of materials, since reaction products are no longer limited by the amount of radicals being dragged and dropped using the tip of an AFM. (3) It expands the concept of on-surface synthesis to organo-halogen-functionalized nanoparticles, whose prospects range from molecular self assembly[24,25] to enhancement of X-ray computed tomography (CT) scans.[26] In general, the technique delivers Nps functionalized with a new covalent organic network cover, which is a new class of organic materials. In addition, we aimed to transfer parameters that control on-surface syntheses on highly controlled surfaces under high vacuum to Np in solution. Furthermore, we investigated parameters that control on-surface syntheses, by a systematic variation of the NHC-coupling precursor, for example, determining the effect of the contact angle of the hybrid material through positioning the halogen in *ortho*-, *meta*- and *para*-positions, probing the effect of the tether length on on-surface Ullmann coupling reactions and exploiting the different reactivities of aryl chlorides, bromides and iodides towards on-surface functionalizations. The devised organic–inorganic hybrid material studied in this work consists of a core, the shell, a binding group, an organic linker, and a reaction partner (Scheme 1). The core of the hybrid material comprises a majority of Au atoms in the oxidation state zero (0). The shell consists of the Au-surface atoms and are directly bound to the organic ligand, in the present case a σ (carbene) electron-donating group.[27] As the orbitals of the metal interact with the ligands, metal–metal interactions are reduced.[27,28] These metal–ligand interactions enhance stabilization and prevent Np agglomeration.[27,29–31] We chose carbenes as organic ligands due to their strong binding to the AuNps similar to the previous system reported by the group of Glorius.[23] More importantly, the tilted geometry of carbenes enables the groups at the wingtip positions to point towards the surface of the Np resulting in an increased proximity of the reacting partners to the surface of the AuNps.[1,3,9,21,32] Therefore, variation of the binding group allows the alteration of the geometry, and hence, the chemical reactivity of the hybrid material. That way, for example, the selectivity of either inter- or intramolecular Ullmann reactions should be controllable. The linker part of the organic ligand separates the AuNp from the aromatic moiety and can be used to effectively tune the distance between the AuNp and the aromatic group.[33–35] Finally, an aryl halide was chosen as the reaction partner for the Ullmann-coupling reaction of the hybrid material, which was functionalized at a suitable position. Putting all these described elements together, **1f-AuNp** was designed as a model system for our on-Np-surface functionalization (Scheme 2). In this case, the organic–inorganic hybrid material performs the function of a catalyst (the AuNp), stabilizing agent (the NHC) and reactant (reaction partner at the wingtip positions) in the investigated Ullmann coupling reactions.

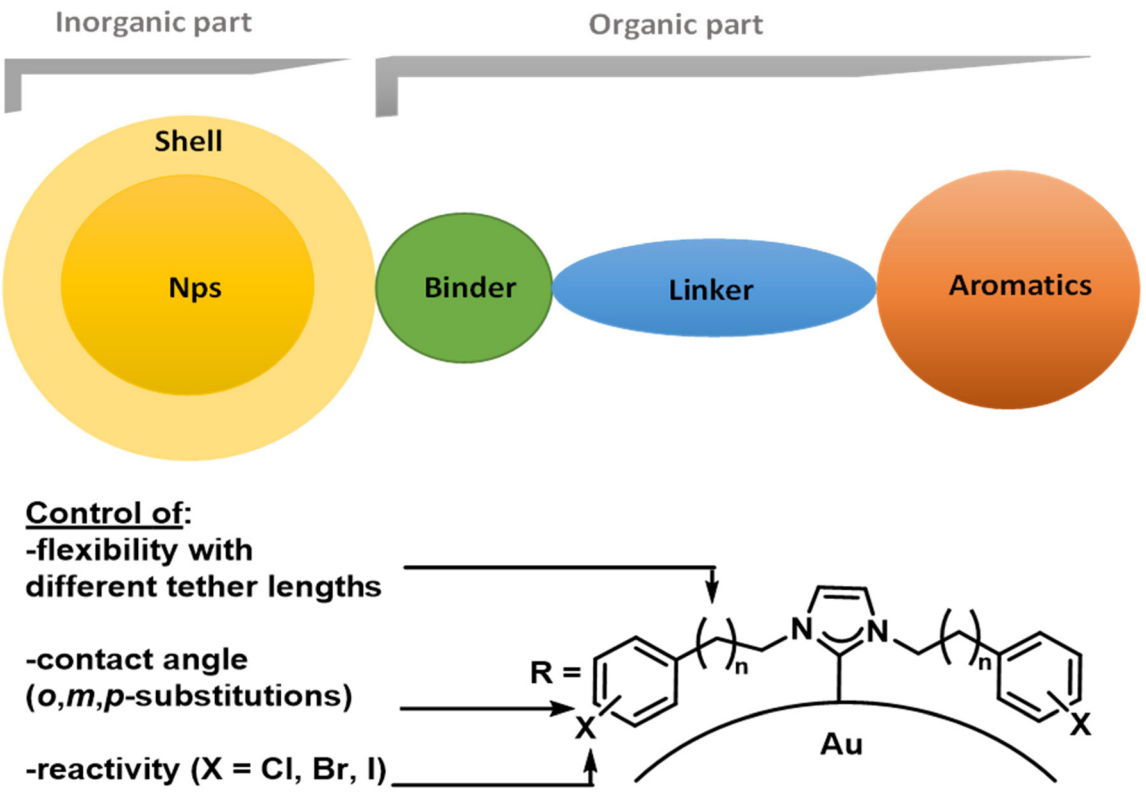

Scheme 1 Schematic representation of the organic–inorganic hybrid material and the different parameters studied in this work.

Open Access Article. Published on 04 September 2024. Downloaded on 5/10/2026 11:54:49 PM.
This article is licensed under a Creative Commons Attribution 3.0 Unported Licence.

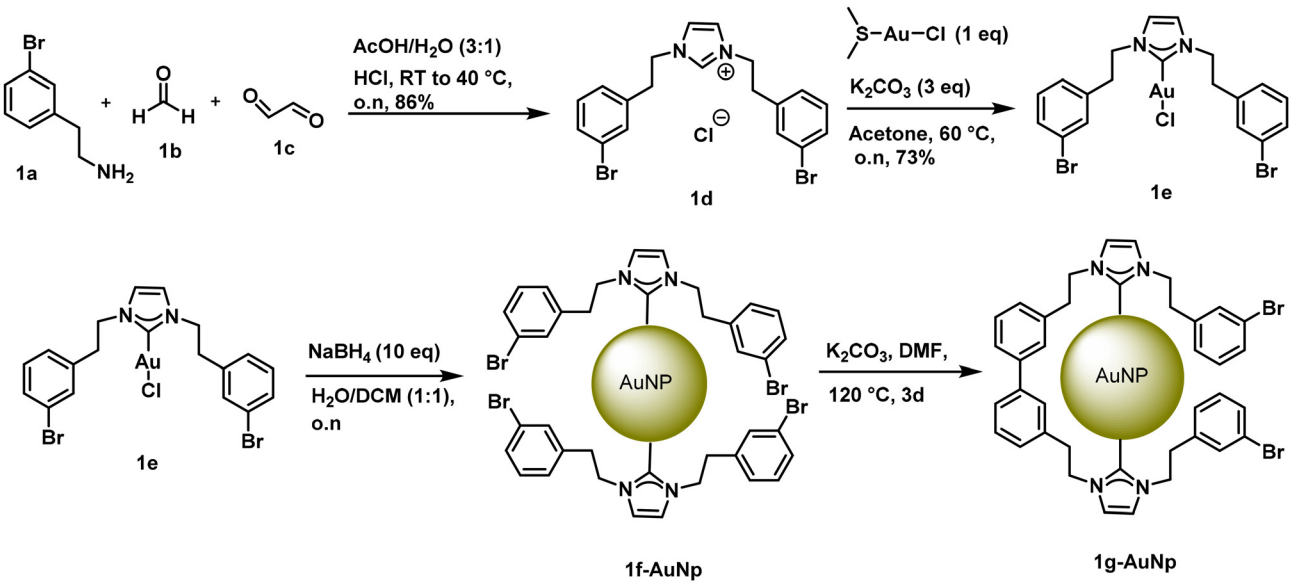

Scheme 2 Syntheses of NHC-functionalized AuNps, **1a** to **1g-AuNp**. For the functionalized Nps (**1f-AuNp** and **1g-AuNp**), a condensed representation depicting two exemplary ligands is shown to illustrate the on-Np-surface reaction.

Results and discussion

Synthesis and characterization of NHC-functionalized AuNps

We envisaged that the retrosynthesis of the target compound **1f-AuNp** could be achieved from a one-pot, three-component Mannich-type reaction of **1a**, **1b** and **1c** as opposed to imidazole alkylations or the use of orthoesters for symmetrical immidazolium salts, as reported in the literature.[36–38] Therefore, we began with two equivalents of **1a** in an AcOH/H_2O mixture (3 : 1) and introduced one equivalent of **1b** to form the corresponding diamine.[37] We then added one equivalent of **1c** to close the ring (Scheme 2). The addition of 3 M HCl and heating the reaction to 40 °C furnished the imidazolium compound **1d** in 86% yield. The ^{1}H-NMR spectrum of **1d** showed a diagnostic singlet at 10.26 ppm corresponding to the proton at the C2 position of the imidazolium ring, sandwiched by the two nitrogen atoms. The reaction of **1d** with K_2CO_3 furnished the N-heterocyclic carbene *in situ*, which was trapped with chloro(dimethylsulphide) gold(I) to give **1e** in 73% yield. The formation of **1e** was confirmed by the loss of the singlet for the NHC proton appearing at 10.26 ppm in its ^{1}H-NMR spectrum, accompanied by an emergence of a signal at 183.22 ppm in the ^{13}C-NMR spectrum, corresponding to the carbene carbon atom of the C–Au bond. These two observations are indicative of successful *in situ* carbene generation and coordination to the gold(I) precursor.[39–41] Complex **1e** was reduced to the nanoparticles using a biphasic water/DCM medium as developed by Prezhdo, Brutchey, and co-workers for the synthesis of NHC-stabilized AgNps.[42,43] Unlike the monophasic media, biphasic solvent systems provide a different pathway with different reaction kinetics, in which the reduction of the gold(I) complex takes place slowly, providing uniformly sized AuNps.[39,44] After aqueous workup, the resulting crude AuNps were thoroughly washed with tetrahydrofuran to remove any unbound ligand furnishing **1f-AuNp**.

The functionalized AuNps were characterized using matrix assisted laser desorption ionization mass spectrometry (MALDI-MS), transmission electron microscopy (TEM), dynamic light scattering (DLS), thermogravimetric analysis (TGA), energy dispersive X-ray spectroscopy (EDX) and X-ray diffraction (XRD). Matrix-assisted and/or laser desorption/ionization mass spectrometry (MALDI-MS or LDI-MS) has been proven to be a useful method for the characterization of NHC's on AuNps and, in some cases, shows the abstraction of gold adatoms, giving rise to Au(NHC)$_2$ species.[45–47] Similar results were obtained in the present study: the simulated and experimental MALDI-MS data showed an abstraction of an Au atom which gave rise to the mass peak at 1060.92 corresponding to the Au(NHC)$_2$ motif (Fig. 1a and S11†). This result confirmed that we have not only the AuNps but also the ligands directly attached to the AuNps.

TEM analysis of the resulting Nps revealed the formation of spherical AuNps with an average diameter of 4.1 ± 0.9 nm (Fig. 1b). However, this technique only enables the visualization of the nanoparticles' metallic core and excludes the organic shell of the Nps due to the much lower contrast of the organic shell, relative to the Au core.[40,41,48,49] We thereby employed dynamic light scattering (DLS) to measure the overall hydrodynamic diameter of the functionalized AuNps in dichloromethane (DCM). As shown in Fig. 1c and S5,† the hydrodynamic diameter of the dispersed AuNps in DCM was estimated at ~22.0 nm. This increase in the hydrodynamic diameter is consistent with the fact that DLS measurements take into account the diameter of the gold core, NHC ligands attached to the AuNps, the electrostatic potential generated by the Nps and the entire solvent cage.

This journal is © The Royal Society of Chemistry 2024

Open Access Article. Published on 04 September 2024. Downloaded on 5/10/2026 11:54:49 PM.
This article is licensed under a Creative Commons Attribution 3.0 Unported Licence.

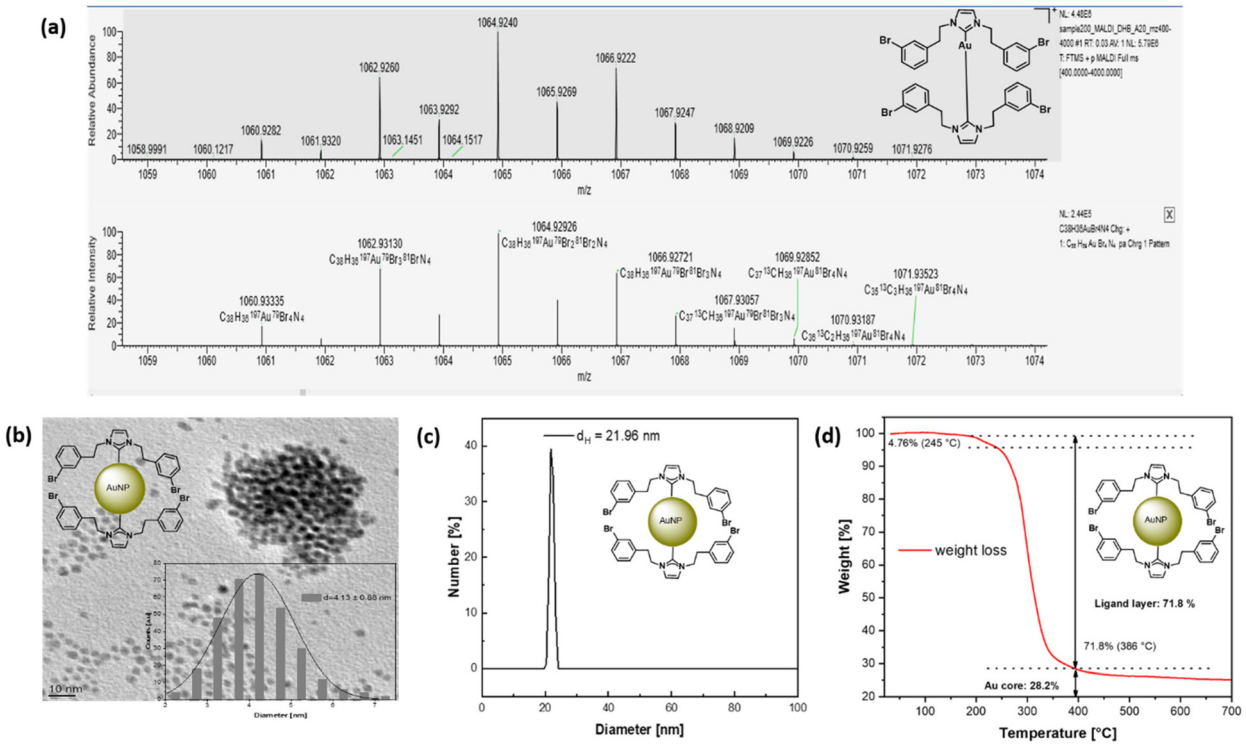

Fig. 1 Characterization of **1f-AuNp**. (a) MALDI-MS spectra of **1f-AuNp**: bottom spectrum: simulated mass spectrum and top spectrum: experimental mass spectrum. Spectra show a mass peak at 1060.9282 (calc. 1060.9333), corresponding to $(NHC)_2Au^+$ fragments, indicating that the ligands are attached to the AuNps. (b) TEM and size distribution (inset) of **1f-AuNp** with an average diameter of 4.1 ± 0.9 nm. (c) DLS spectrum of **1f-AuNp** with a hydrodynamic diameter of 22.0 nm and (d) thermogram of **1f-AuNp**, with an NHC : Au core mass ratio of 72 : 28.

Thermogravimetric analysis (TGA) was used to determine the ratio of Au to NHC ligands in the resulting Nps (Fig. 1d). There was a gradual decomposition at 245 °C, corresponding to 4.76% weight loss of the functionalized Nps. At 248 to 382 °C, there was a massive decomposition corresponding to 71.8% of the entire mass of the Np.

At higher temperatures up to 700 °C, no further phase change was observed indicating a 28.2% composition of the Au core. Taking into account the weight percent of NHC from TGA analysis and the diameter of AuNps from TEM measurements, we were able to calculate the average number of NHCs on each Np following the method employed by Johnson and co-workers.[39] An average number of ≈2680 NHC molecules was present on the surface of the AuNp. Note that the NHC/**1f-AuNp** value might be inflated as it depends on the number of Au atoms in the Np, and the calculation of the number of Au atoms assumes a smooth spherical particle.[39] Nevertheless, this value indicates a high coverage of NHC per AuNp, as opposed to single molecules reported on a planar 2D Au surface.[22,23] In addition, the calculated value is in excellent agreement with literature reports for NHC-functionalized AuNps of similar core sizes.[28,39–41,44,48,50]

We employed energy dispersive X-ray spectroscopy (EDX) to determine the chemical composition of the AuNps. Peaks at 0.20, 0.24, 1.45 and 2.20 keV correspond to C Kα, N Kα, Br Lα, and Au Mα, respectively (Fig. S7†). Additionally, the X-ray diffraction (XRD) profiles of the AuNps (Fig. S9†) showed reflexes at 38.5, 44.3, 64.5, and 77.7°, corresponding to the Au (111), (200), (220), and (311) lattice planes of Au, thus, indicating that the synthesized Nps are constructed from Au atoms.[51]

Ullmann coupling reaction on the surface of AuNps

As mentioned above, the design of the presented organic–inorganic hybrid system combines the coupling partners, catalyst and reducing agent, all in one entity, with the aryl halides close to the surface of the Np.[27,32,52–54] Recent work by Camden and coworkers has shown that the geometry of these NHCs on nanoparticles is not far off from that on a 2D surface, and they rather exist in both flat and vertical configurations.[53] However, a linker molecule provides suitable distance between the aromatics and the AuNps. Several functional groups have been employed as linker molecules, but these functional groups have to be chemically inert towards the exact application of the hybrid material.[33–35,55,56] Moreover, a linker should be of optimum length, which minimizes electronic and steric effects between the AuNps and the aromatic moiety, while also enabling desired flexibility and motion of the entire ligand – that allows on-surface reactivity – when attached to the AuNps. We thereby settled for an ethylene chain as a linker, since it is chemically inert under Ullmann conditions, provides a suitable distance between the AuNps and the aromatic moiety, and in turn, avoids the flipping away

Open Access Article. Published on 04 September 2024. Downloaded on 5/10/2026 11:54:49 PM.
This article is licensed under a Creative Commons Attribution 3.0 Unported Licence.

of the reacting partner, which arises from a high degree of flexibility of ligands with long chain lengths, when attached to the Nps.[56,57]

With these criteria in mind, we selected **1f-AuNp**, which has a linker of two carbon atoms, with the bromine situated at the *meta*-position (Fig. 2). Accordingly, the reaction of **1f-AuNp** with 12 equivalents of K_2CO_3 furnished **1g-AuNp**. We employed attenuated total reflectance infrared spectroscopy (ATR-IR) and surface enhanced Raman spectroscopy (SERS) to analyze the successful coupling reaction on the surface of AuNps, which were used in characterizing similar hybrid systems.[32,39,41,48,53,54,58,59] IR spectra showed a strong reduction in the intensity of the band at 1070 cm^{-1}, which is assigned to the C–Br vibration frequency. This decrease indicates that some of the C–Br bonds have been replaced by another, a C–C bond (Fig. 3a). The rest of the spectrum was unperturbed, indicating that the functionalized AuNp was only modified at the bromine position. In addition, SERS spectra showed a complete disappearance of the band at 665 cm^{-1} (C–Br bond), relative to the SERS spectrum before the reaction.

EDX analysis of the reacted Np showed a 10.5% increase in the C composition of the sample, 11.7% decrease in Br composition, and a corresponding 0.3% decrease in Au composition (Fig. S7 and S8†). These observations are also in accordance with a coupling reaction at the C–Br bond since Ullmann reaction is driven by the leaching of Au to AuBr. The loss of Au in Ullmann reaction has been observed and reported in the literature. For example, the group of Kantam observed 9.5% leaching of Au with a significant decrease in yield after three cycles of Ullmann reactions.[60] Similarly, the group of Jin also saw

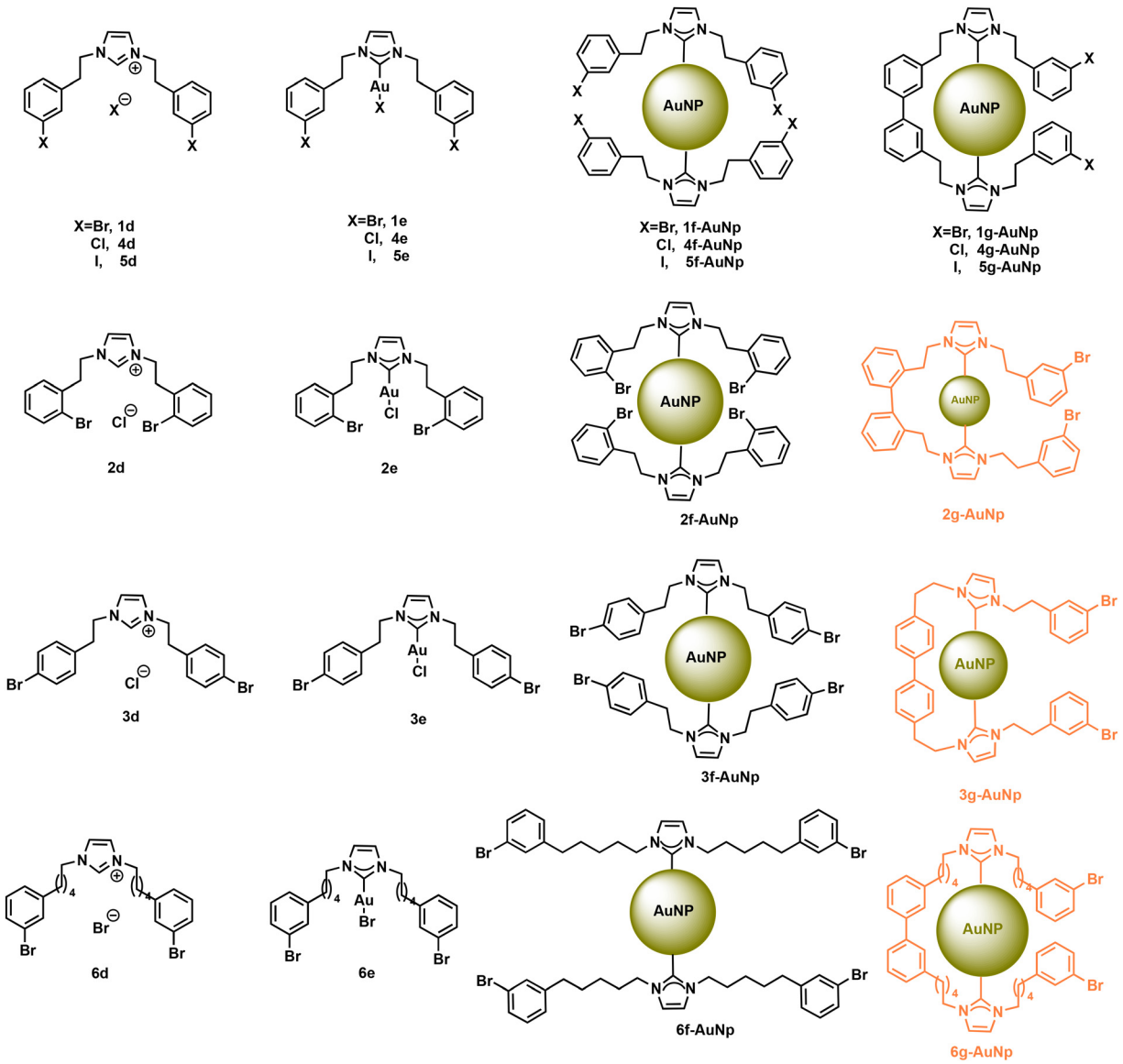

Fig. 2 N-Heterocyclic carbenes studied in this work. The compounds marked in black were successfully synthesized, while those marked in red did not undergo on-surface Ullmann coupling reactions.

This journal is © The Royal Society of Chemistry 2024

Open Access Article. Published on 04 September 2024. Downloaded on 5/10/2026 11:54:49 PM.
This article is licensed under a Creative Commons Attribution 3.0 Unported Licence.

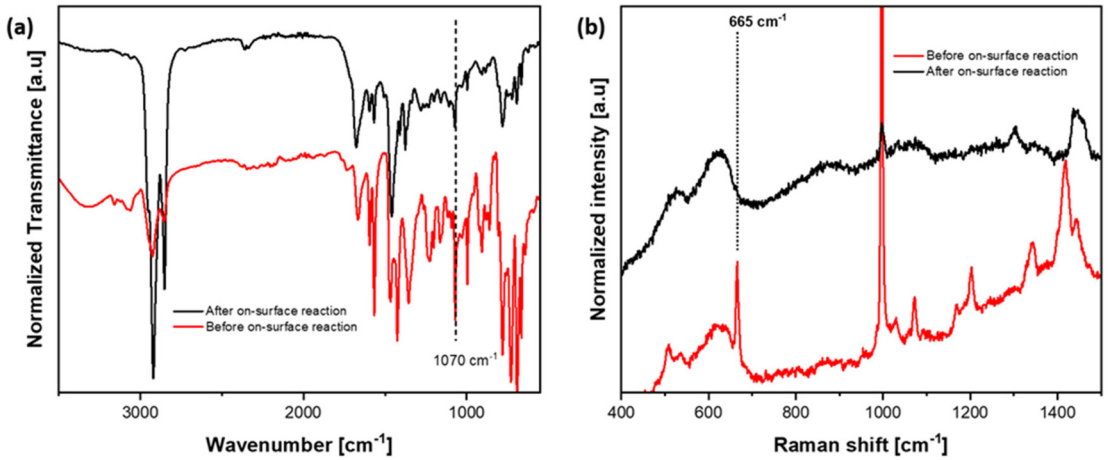

Fig. 3 Ullmann coupling of **1f-AuNp**. (a) IR spectra and (b) SERS spectra AuNps before the reaction (red) and after the Ullmann reaction (black).

leaching of Au in Ullmann reaction and a reduced yield after about five cycles.[61] Moreover, the observation that bromine can still be traced in the composition of **1g-AuNp** suggests that the reaction did not reach 100% conversion. It contained both the reacted and the unreacted ligands, attached to the same surface of the AuNp. However, the formation of aryl–Au bonds *via* oxidative addition is rather unlikely, as several reports have shown that in Au-promoted Ullmann reactions, the process does not stop at the stage of oxidative addition. In this case, the cycle of reductive elimination is completed and eventually the C–C coupling product is formed.[61–65]

Furthermore, the on-Np-surface coupling reaction was confirmed using MALDI-MS. MALDI-MS spectra showed a mass peak at 903.09 corresponding to the mass of **1g-AuNp** with an abstraction of an Au atom in the form of the $Au(NHC)_2$ motif, just as expected (Fig. S13†), thus indicating that the successful on-surface reaction of the aryl moiety of **1f-AuNp** was achieved. This spectrum was also in perfect agreement with the calculated spectrum for the proposed structure on the surface of the AuNp (Fig. S13†). In addition, we observed a MALDI mass peak of two coupled units with two open ring dimers, which corresponds to the reduction of the C–Br band observed in the SERS and IR spectra (Fig. S14†). This result supports that the on-Np-surface reaction is not limited to two coupling units but can exist in a chain-like manner, leading to multiple coupled units on the surface of the AuNps. Nonetheless, MALDI analyses of **1g-AuNp** also showed the mass of the starting material as 432.99 (Fig. S12†) corresponding to the mass observed in the ESI-MS of **Id** (page S4†). These data also corroborate the results of EDX spectroscopy, which allude that the reacted nanoparticles comprise both reacted and unreacted NHC-ligands bound to the same surface of the AuNp.

Next, we attempted an intermolecular hetero-Ullmann coupling of compound **1f-AuNp** with *p*-bromobenzonitrile under the same reaction conditions for the intramolecular homo-Ullmann reaction. However, there was no evidence for a hetero-coupling reaction between **1f-AuNp** and *p*-bromobenzonitrile, suggesting that the tilted geometry of the carbenes leads preferably to an intramolecular homo-Ullmann reaction over intermolecular hetero-Ullmann reaction.

We then probed how the proximity of the halogen towards the surface of AuNps influences on-Np-surface Ullmann reaction, by varying the Br substitution from *meta* to *ortho* and *para* positions, and repeated the Ullmann reactions with the above conditions applied for **1f-AuNp**. However, we were unable to obtain the expected products (**2g-AuNp** and **3g-AuNp**). SERS of **3g-AuNp** and ATR-IR spectroscopy of **2g-AuNp** showed a reasonable retention of the starting material, with SERS bands at 631, 770 and 1071 cm^{-1} (Fig. S21†), corresponding to the C–Br bond, C–C aliphatic chain at the wingtip position, and benzene groups, respectively. This result can be rationalized as the two Br atoms from two adjacent aryl units need to be in proximity with the Au surface to enable an oxidative addition followed by a reductive elimination, which then furnishes the coupled product on the Np. In the case of **2f-AuNp** and **3f-AuNp**, the geometry does not fit and no insertion can occur.

Additionally, we tested the reactivities of different halogens towards on-Np-surface coupling reactions by varying the halogen from Br to Cl and I. Applying the same reaction conditions, we were unable to obtain the desired coupling products, **4g-AuNp** and **5g-AuNp**. The SERS spectrum of **5g-AuNp** deviated from that of the starting material, **5f-AuNp** (Fig. S22†). There was a significant intensification of C–C aliphatic chains due to the pronounced band at 733 cm^{-1}. In addition, there was a slight retention of aromatic rings due to the band at 998 cm^{-1}. These two concurrent observations indicate a degradation of **5f-AuNp** at the reaction temperature. In addition, the ATR-IR spectrum of **5g-AuNp** showed significant broadening of the signals and appearance of new bands relative to the starting material (Fig. S18†), bolstering the conclusion from the SERS data. This is plausible, as aryl iodides have been reported to be more reactive than their bromide and chloride counterparts, requiring lower temperatures of

Open Access Article. Published on 04 September 2024. Downloaded on 5/10/2026 11:54:49 PM. This article is licensed under a Creative Commons Attribution 3.0 Unported Licence.

activation in the in-solution and on-surface coupling reactions.[66] To also validate this known phenomenon for on-Np-surface reactivity, we repeated the on-surface Ullmann reaction of **5f-AuNp** while reducing the reaction temperature from 120 to 100 °C. Under these conditions, we were able to obtain **5g-AuNp**, whose coupling product is essentially the same as that obtained from the previously studied precursor, **1f-AuNp** (Fig. S20†).

Also, for **4f-AuNp**, no coupling was observed. This is expected and in accordance with the lower reactivity of aryl chlorides. Interestingly, the TEM analysis of **4f-AuNp** showed deviation from the other Nps, such as a lack of size uniformities, slight distortion in core shapes and increased diameters of these Nps with an average Au core size of 35 ± 24 nm (Fig. S3†). Therefore, this behavior could not be excluded to explain the unsuccessful formation of **4g-AuNp**, since surface reaction and surface catalysis are dependent on shapes, sizes, porosity, diffusion rates and surface areas of Nps.[67]

Next, we studied how the orientation of the entire reaction partner towards the AuNp influences reactivity on the Np-surfaces. We varied the length of the linker from C_2 to C_5 and repeated the same Ullmann reaction. Again, we were unable to obtain the coupling product **6g-AuNp** from **6f-AuNp**. This can be attributed to the fact that the coupling partners are too flexible and can flip away from the surface of the Np to minimize sterics, which in turn, minimizes the proximity between the aryl halide moiety and the surface of the AuNp. In addition, it has been established that NHC ligands can move easily on surfaces *via* a unique ballbot-type motion, in which the NHC first pulls out an Au adatom (as also observed in this study), and then rides on it across the surface.[23,32,54,68] This distinctive mode of mobility is fundamental to the formation of surface assembled monolayers (SAMs). This ballbot-type motion is more and more hindered as the ligand size increases and is, therefore, a function of the ligand size and ligand electronics.[23,68] Thus, a combination of the aforementioned effects can rationalize the lack of reactivity of **6f-AuNp** towards Ullmann reaction.

We proceeded with further characterization of the successfully functionalized AuNp (that is **1g-AuNp**) to determine the nature and/or existence of the nanoparticles after on-Np-surface Ullmann reaction. TEM showed an increase in core sizes with an average core size of 17 ± 9 nm (Fig. S4†). Additionally, the DLS spectrum of **1g-AuNp** (Fig. S6†) revealed a hydrodynamic diameter of 33.8 nm with a zeta potential value of 0.180 mV, which is suggestive of a neutrally charged ligand and a tendency of precipitation when dispersed in CH_2Cl_2. EDX analyses of **1g-AuNp** showed an Au Mα signal at 2.2 keV, indicating the retention of the AuNps after the reaction. In addition, the XRD profile of the reacted AuNps showed reflexes at 38.5, 44.3, 64.5, and 77.7°, which correlate with the face-centered cubic unit cell of AuNps. It is noteworthy to mention that the XRD reflexes became more pronounced relative to the AuNp prior to the on-surface reaction. This phenomenon is due to an increase in sizes, as the reflexes due to AuNps become relatively more pronounced in this size regime.[51] This observation is in accordance with the result of the TEM and DLS measurements. The abstraction of an Au adatom by the reacted ligands – which was observed by MALDI MS experiments – also suggests the retention of these Nps after being subjected to Ullmann reaction conditions. All data point to the fact that the nanoparticles still remained as nanoparticles after having undergone a successful on-surface Ullmann reaction.

Conclusion

By varying the planar 2D surfaces of gold(111) to a rough surface of gold nanoparticles and fine-tuning the different segments of a hybrid material, we were able to utilize the bonding geometry of NHCs on AuNps to successfully achieve an Ullmann coupling of aryl halide moieties connected *via* NHC on a one-system hybrid material functioning as the catalyst and reacting partner. The synthesis of the nanoparticles was characterized by a combination of MALDI-MS, TEM, DLS, TGA, zeta potential value measurements, EDX, and XRD. While reactions and retention of the nanoparticles were confirmed by a combination of IR, SERS, EDX, MALDI-MS, XRD, TEM, and DLS, we studied how the nature and proximity of the halogen and that of the reacting partner to the surface of the Nps influenced the reactivity on surfaces. Our work supports that an appropriate organic ligand, suitable halogen position, moderate chain length, and moderate reactivity of halogen are influential towards the selectivities of Ullmann coupling on AuNps, thus, opening new prospects in organic on-surface synthesis to a promising class of organic–metal hybrid materials.

Data availability

General information, synthetic procedure, TEM, DLS, and EDX analysis results, XRD patterns, MALDI spectra, ATR-IR, SERS, and NMR spectra, and additional references are provided in the ESI.†

Author contributions

H. A. Wegner conceptualized the project and interpreted the data. N. Ukah modified the concept, implemented it, conducted all experiments, interpreted the data and analyzed all results. Both authors were involved in the manuscript preparation.

Conflicts of interest

There are no conflicts to declare.

 This journal is © The Royal Society of Chemistry 2024

Open Access Article. Published on 04 September 2024. Downloaded on 5/10/2026 11:54:49 PM. This article is licensed under a Creative Commons Attribution 3.0 Unported Licence.

Acknowledgements

This work was supported by the LOEWE Program of Excellence of the Federal State of Hesse (LOEWE Focus Group PriOSS 'Principles of On-Surface Synthesis') and Justus Liebig University, Giessen, Germany. In addition, the authors wish to express their sincere gratitude to Anne Schulze, Limei Chen, Max Müller, Klaus Peppler and Christian Bauer for the TEM, SERS, MALDI, EDX and XRD measurements.

References

1 A. V. Zhukhovitskiy, M. J. MacLeod and J. A. Johnson, Carbene Ligands in Surface Chemistry: From Stabilization of Discrete Elemental Allotropes to Modification of Nanoscale and Bulk Substrates, *Chem. Rev.*, 2015, **115**, 11503–11532.

2 C.-Y. Wu, W. J. Wolf, Y. Levartovsky, H. A. Bechtel, M. C. Martin, F. D. Toste and E. Gross, High-spatial-resolution mapping of catalytic reactions on single particles, *Nature*, 2017, **541**, 511–515.

3 C. A. Smith, M. R. Narouz, P. A. Lummis, I. Singh, A. Nazemi, C.-H. Li and C. M. Crudden, N-Heterocyclic Carbenes in Materials Chemistry, *Chem. Rev.*, 2019, **119**, 4986–5056.

4 K. A. Simonov, N. A. Vinogradov, A. S. Vinogradov, A. V. Generalov, E. M. Zagrebina, G. I. Svirskiy, A. A. Cafolla, T. Carpy, J. P. Cunniffe, T. Taketsugu, A. Lyalin, N. Mårtensson and A. B. Preobrajenski, From Graphene Nanoribbons on Cu(111) to Nanographene on Cu(110): Critical Role of Substrate Structure in the Bottom-Up Fabrication Strategy, *ACS Nano*, 2015, **9**, 8997–9011.

5 Q. Shen, H.-Y. Gao and H. Fuchs, Frontiers of on-surface synthesis: From principles to applications, *Nano Today*, 2017, **13**, 77–96.

6 P. Ruffieux, S. Wang, B. Yang, C. Sánchez-Sánchez, J. Liu, T. Dienel, L. Talirz, P. Shinde, C. A. Pignedoli, D. Passerone, T. Dumslaff, X. Feng, K. Müllen and R. Fasel, On-surface synthesis of graphene nanoribbons with zigzag edge topology, *Nature*, 2016, **531**, 489–492.

7 R. Pawlak, X. Liu, S. Ninova, P. D'Astolfo, C. Drechsel, S. Sangtarash, R. Häner, S. Decurtins, H. Sadeghi, C. J. Lambert, U. Aschauer, S.-X. Liu and E. Meyer, Bottom-up Synthesis of Nitrogen-Doped Porous Graphene Nanoribbons, *J. Am. Chem. Soc.*, 2020, **142**, 12568–12573.

8 J. C. Love, L. A. Estroff, J. K. Kriebel, R. G. Nuzzo and G. M. Whitesides, Self-assembled monolayers of thiolates on metals as a form of nanotechnology, *Chem. Rev.*, 2005, **105**, 1103–1169.

9 M. Koy, P. Bellotti, M. Das and F. Glorius, N-Heterocyclic carbenes as tunable ligands for catalytic metal surfaces, *Nat. Catal.*, 2021, **4**, 352–363.

10 C. J. Judd, F. L. Q. Junqueira, S. L. Haddow, N. R. Champness, D. A. Duncan, R. G. Jones and A. Saywell, Structural characterisation of molecular conformation and the incorporation of adatoms in an on-surface Ullmann-type reaction, *Commun. Chem.*, 2020, **3**, 166.

11 L. Grossmann, D. A. Duncan, S. P. Jarvis, R. G. Jones, S. De, J. Rosen, M. Schmittel, W. M. Heckl, J. Björk and M. Lackinger, Evolution of adsorption heights in the on-surface synthesis and decoupling of covalent organic networks on Ag(111) by normal-incidence X-ray standing wave, *Nanoscale Horiz.*, 2021, **7**, 51–62.

12 L. Grill and S. Hecht, Covalent on-surface polymerization, *Nat. Chem.*, 2020, **12**, 115–130.

13 M. Fritton, D. A. Duncan, P. S. Deimel, A. Rastgoo-Lahrood, F. Allegretti, J. V. Barth, W. M. Heckl, J. Björk and M. Lackinger, The Role of Kinetics versus Thermodynamics in Surface-Assisted Ullmann Coupling on Gold and Silver Surfaces, *J. Am. Chem. Soc.*, 2019, **141**, 4824–4832.

14 J. Eichhorn, D. Nieckarz, O. Ochs, D. Samanta, M. Schmittel, P. J. Szabelski and M. Lackinger, On-surface Ullmann coupling: the influence of kinetic reaction parameters on the morphology and quality of covalent networks, *ACS Nano*, 2014, **8**, 7880–7889.

15 M. Di Giovannantonio, M. Tomellini, J. Lipton-Duffin, G. Galeotti, M. Ebrahimi, A. Cossaro, A. Verdini, N. Kharche, V. Meunier, G. Vasseur, Y. Fagot-Revurat, D. F. Perepichka, F. Rosei and G. Contini, Mechanistic Picture and Kinetic Analysis of Surface-Confined Ullmann Polymerization, *J. Am. Chem. Soc.*, 2016, **138**, 16696–16702.

16 M. Di Giovannantonio, M. El Garah, J. Lipton-Duffin, V. Meunier, L. Cardenas, Y. Fagot Revurat, A. Cossaro, A. Verdini, D. F. Perepichka, F. Rosei and G. Contini, Insight into organometallic intermediate and its evolution to covalent bonding in surface-confined ullmann polymerization, *ACS Nano*, 2013, **7**, 8190–8198.

17 C. M. Crudden, J. H. Horton, M. R. Narouz, Z. Li, C. A. Smith, K. Munro, C. J. Baddeley, C. R. Larrea, B. Drevniok, B. Thanabalasingam, A. B. McLean, O. V. Zenkina, I. I. Ebralidze, Z. She, H.-B. Kraatz, N. J. Mosey, L. N. Saunders and A. Yagi, Simple direct formation of self-assembled N-heterocyclic carbene monolayers on gold and their application in biosensing, *Nat. Commun.*, 2016, **7**, 12654.

18 C. M. Crudden, J. H. Horton, I. I. Ebralidze, O. V. Zenkina, A. B. McLean, B. Drevniok, Z. She, H.-B. Kraatz, N. J. Mosey, T. Seki, E. C. Keske, J. D. Leake, A. Rousina-Webb and G. Wu, Ultra stable self-assembled monolayers of N-heterocyclic carbenes on gold, *Nat. Chem.*, 2014, **6**, 409–414.

19 S. Clair and D. G. de Oteyza, Controlling a Chemical Coupling Reaction on a Surface: Tools and Strategies for On-Surface Synthesis, *Chem. Rev.*, 2019, **119**, 4717–4776.

20 P. Bellotti, M. Koy, M. N. Hopkinson and F. Glorius, Recent advances in the chemistry and applications of N-heterocyclic carbenes, *Nat. Rev. Chem.*, 2021, **5**, 711–725.

21 S. Amirjalayer, A. Bakker, M. Freitag, F. Glorius and H. Fuchs, Cooperation of N-Heterocyclic Carbenes on a Gold Surface, *Angew. Chem., Int. Ed.*, 2020, **59**, 21230–21235.

Open Access Article. Published on 04 September 2024. Downloaded on 5/10/2026 11:54:49 PM. This article is licensed under a Creative Commons Attribution 3.0 Unported Licence.

22 Q. Zhong, A. Ihle, S. Ahles, H. A. Wegner, A. Schirmeisen and D. Ebeling, Constructing covalent organic nanoarchitectures molecule by molecule via scanning probe manipulation, *Nat. Chem.*, 2021, **13**, 1133–1139.

23 J. Ren, M. Koy, H. Osthues, B. S. Lammers, C. Gutheil, M. Nyenhuis, Q. Zheng, Y. Xiao, L. Huang, A. Nalop, Q. Dai, H.-J. Gao, H. Mönig, N. L. Doltsinis, H. Fuchs and F. Glorius, On-surface synthesis of ballbot-type N-heterocyclic carbene polymers, *Nat. Chem.*, 2023, **15**, 1737–1744.

24 T. Shirman, R. Kaminker, D. Freeman and M. E. van der Boom, Halogen-bonding mediated stepwise assembly of gold nanoparticles onto planar surfaces, *ACS Nano*, 2011, **5**, 6553–6563.

25 K. Buntara Sanjeeva, C. Pigliacelli, L. Gazzera, V. Dichiarante, F. Baldelli Bombelli and P. Metrangolo, Halogen bond-assisted self-assembly of gold nanoparticles in solution and on a planar surface, *Nanoscale*, 2019, **11**, 18407–18415.

26 S.-H. Kim, E.-M. Kim, C.-M. Lee, D. W. Kim, S. T. Lim, M.-H. Sohn and H.-J. Jeong, Synthesis of PEG–Iodine–Capped Gold Nanoparticles and Their Contrast Enhancement in In Vitro and In Vivo for X–Ray/CT, *J. Nanomater.*, 2012, **2012**, 504026–504034.

27 Y. Kim, S. Ji and J.-M. Nam, A Chemist's View on Electronic and Steric Effects of Surface Ligands on Plasmonic Metal Nanostructures, *Acc. Chem. Res.*, 2023, **56**, 2139–2150.

28 M. W. Brett, C. K. Gordon, J. Hardy and N. J. L. K. Davis, The Rise and Future of Discrete Organic-Inorganic Hybrid Nanomaterials, *ACS Phys. Chem. Au*, 2022, **2**, 364–387.

29 D. A. Hines and P. V. Kamat, Recent advances in quantum dot surface chemistry, *ACS Appl. Mater. Interfaces*, 2014, **6**, 3041–3057.

30 L. M. Rossi, J. L. Fiorio, M. A. S. Garcia and C. P. Ferraz, The role and fate of capping ligands in colloidally prepared metal nanoparticle catalysts, *Dalton Trans.*, 2018, **47**, 5889–5915.

31 J. de Roo, M. Ibáñez, P. Geiregat, G. Nedelcu, W. Walravens, J. Maes, J. C. Martins, I. van Driessche, M. V. Kovalenko and Z. Hens, Highly Dynamic Ligand Binding and Light Absorption Coefficient of Cesium Lead Bromide Perovskite Nanocrystals, *ACS Nano*, 2016, **10**, 2071–2081.

32 S. Dery, W. Cao, C. Yao and C. Copéret, NMR Spectroscopic Signatures of Cationic Surface Sites from Supported Coinage Metals Interacting with N-Heterocyclic Carbenes, *J. Am. Chem. Soc.*, 2024, 6466–6470.

33 Z. Huang and M. L. Tang, Designing Transmitter Ligands That Mediate Energy Transfer between Semiconductor Nanocrystals and Molecules, *J. Am. Chem. Soc.*, 2017, **139**, 9412–9418.

34 Z. Huang, Z. Xu, T. Huang, V. Gray, K. Moth-Poulsen, T. Lian and M. L. Tang, Evolution from Tunneling to Hopping Mediated Triplet Energy Transfer from Quantum Dots to Molecules, *J. Am. Chem. Soc.*, 2020, **142**, 17581–17588.

35 X. Li, Z. Huang, R. Zavala and M. L. Tang, Distance-Dependent Triplet Energy Transfer between CdSe Nanocrystals and Surface Bound Anthracene, *J. Phys. Chem. Lett.*, 2016, **7**, 1955–1959.

36 L. Benhamou, E. Chardon, G. Lavigne, S. Bellemin-Laponnaz and V. César, Synthetic routes to N-heterocyclic carbene precursors, *Chem. Rev.*, 2011, **111**, 2705–2733.

37 M. H. Dunn, N. Konstandaras, M. L. Cole and J. B. Harper, Targeted and Systematic Approach to the Study of pKa Values of Imidazolium Salts in Dimethyl Sulfoxide, *J. Org. Chem.*, 2017, **82**, 7324–7331.

38 K. M. Kuhn and R. H. Grubbs, A facile preparation of imidazolinium chlorides, *Org. Lett.*, 2008, **10**, 2075–2077.

39 M. J. MacLeod and J. A. Johnson, PEGylated N-Heterocyclic Carbene Anchors Designed To Stabilize Gold Nanoparticles in Biologically Relevant Media, *J. Am. Chem. Soc.*, 2015, **137**, 7974–7977.

40 N. A. Nosratabad, Z. Jin, L. Du, M. Thakur and H. Mattoussi, N-Heterocyclic Carbene-Stabilized Gold Nanoparticles: Mono- Versus Multidentate Ligands, *Chem. Mater.*, 2021, **33**, 921–933.

41 M. Bélanger-Bouliga, R. Mahious, P. I. Pitroipa and A. Nazemi, Perylene diimide-tagged N-heterocyclic carbene-stabilized gold nanoparticles: How much ligand desorbs from surface in presence of thiols?, *Dalton Trans.*, 2021, **50**, 5598–5606.

42 H. Lu and R. L. Brutchey, Tunable Room-Temperature Synthesis of Coinage Metal Chalcogenide Nanocrystals from N -Heterocyclic Carbene Synthons, *Chem. Mater.*, 2017, **29**, 1396–1403.

43 H. Lu, Z. Zhou, O. V. Prezhdo and R. L. Brutchey, Exposing the Dynamics and Energetics of the N-Heterocyclic Carbene-Nanocrystal Interface, *J. Am. Chem. Soc.*, 2016, **138**, 14844–14847.

44 M. R. Narouz, C.-H. Li, A. Nazemi and C. M. Crudden, Amphiphilic N-Heterocyclic Carbene-Stabilized Gold Nanoparticles and Their Self-Assembly in Polar Solvents, *Langmuir*, 2017, **33**, 14211–14219.

45 N. L. Dominique, I. M. Jensen, G. Kaur, C. Q. Kotseos, W. C. Boggess, D. M. Jenkins and J. P. Camden, Giving Gold Wings: Ultrabright and Fragmentation Free Mass Spectrometry Reporters for Barcoding, Bioconjugation Monitoring, and Data Storage, *Angew. Chem., Int. Ed.*, 2023, **62**, e202219182.

46 N. L. Dominique, S. L. Strausser, J. E. Olson, W. C. Boggess, D. M. Jenkins and J. P. Camden, Probing N-Heterocyclic Carbene Surfaces with Laser Desorption Ionization Mass Spectrometry, *Anal. Chem.*, 2021, **93**, 13534–13538.

47 G. Kaur, N. L. Dominique, G. Hu, P. Nalaoh, R. L. Thimes, S. L. Strausser, L. Jensen, J. P. Camden and D. M. Jenkins, Reactivity variance between stereoisomers of saturated N-heterocyclic carbenes on gold surfaces, *Inorg. Chem. Front.*, 2023, **10**, 6282–6293.

48 J. F. DeJesus, L. M. Sherman, D. J. Yohannan, J. C. Becca, S. L. Strausser, L. F. P. Karger, L. Jensen, D. M. Jenkins and

 This journal is © The Royal Society of Chemistry 2024

Open Access Article. Published on 04 September 2024. Downloaded on 5/10/2026 11:54:49 PM. This article is licensed under a Creative Commons Attribution 3.0 Unported Licence.

J. P. Camden, A Benchtop Method for Appending Protic Functional Groups to N–Heterocyclic Carbene Protected Gold Nanoparticles, *Angew. Chem.*, 2020, **132**, 7655–7660.

49 E. L. Albright, T. I. Levchenko, V. K. Kulkarni, A. I. Sullivan, J. F. DeJesus, S. Malola, S. Takano, M. Nambo, K. Stamplecoskie, H. Häkkinen, T. Tsukuda and C. M. Crudden, N-Heterocyclic Carbene-Stabilized Atomically Precise Metal Nanoclusters, *J. Am. Chem. Soc.*, 2024, **146**, 5759–5780.

50 T. C. Jones, L. Sumner, G. Ramakrishna, M. B. Hatshan, A. Abuhagr, S. Chakraborty and A. Dass, Bulky t -Butyl Thiolated Gold Nanomolecular Series: Synthesis, Characterization, Optical Properties, and Electrocatalysis, *J. Phys. Chem.*, 2018, **122**, 17726–17737.

51 S. Krishnamurthy, A. Esterle, N. C. Sharma and S. V. Sahi, Yucca-derived synthesis of gold nanomaterial and their catalytic potential, *Nanoscale Res. Lett.*, 2014, **9**, 627.

52 G. Kaur, R. L. Thimes, J. P. Camden and D. M. Jenkins, Fundamentals and applications of N-heterocyclic carbene functionalized gold surfaces and nanoparticles, *Chem. Commun.*, 2022, **58**, 13188–13197.

53 R. L. Thimes, A. V. B. Santos, R. Chen, G. Kaur, L. Jensen, D. M. Jenkins and J. P. Camden, Using Surface-Enhanced Raman Spectroscopy to Unravel the Wingtip-Dependent Orientation of N-Heterocyclic Carbenes on Gold Nanoparticles, *J. Phys. Chem. Lett.*, 2023, **14**, 4219–4224.

54 J. M. Palasz, Z. Long, J. Meng, P. E. Videla, H. R. Kelly, T. Lian, V. S. Batista and C. P. Kubiak, A Resilient Platform for the Discrete Functionalization of Gold Surfaces Based on N-Heterocyclic Carbene Self-Assembled Monolayers, *J. Am. Chem. Soc.*, 2024, **146**, 10489–10497.

55 V. Gray, Z. Zhang, S. Dowland, J. R. Allardice, A. M. Alvertis, J. Xiao, N. C. Greenham, J. E. Anthony and A. Rao, Thiol-Anchored TIPS-Tetracene Ligands with Quantitative Triplet Energy Transfer to PbS Quantum Dots and Improved Thermal Stability, *J. Phys. Chem. Lett.*, 2020, **11**, 7239–7244.

56 C. Xia, W. Wang, L. Du, F. T. Rabouw, D. V. D. J. Heuvel, H. C. Gerritsen, H. Mattoussi and C. de Mello Donega, Förster Resonance Energy Transfer between Colloidal CuInS 2 /ZnS Quantum Dots and Dark Quenchers, *J. Phys. Chem.*, 2020, **124**, 1717–1731.

57 A. Rossi, M. B. Price, J. Hardy, J. Gorman, T. W. Schmidt and N. J. L. K. Davis, Energy Transfer between Perylene Diimide Based Ligands and Cesium Lead Bromide Perovskite Nanocrystals, *J. Phys. Chem.*, 2020, **124**, 3306–3313.

58 L. M. Sherman, M. D. Finley, R. K. Borsari, N. Schuster-Little, S. L. Strausser, R. J. Whelan, D. M. Jenkins and J. P. Camden, N-Heterocyclic Carbene Ligand Stability on Gold Nanoparticles in Biological Media, *ACS Omega*, 2022, **7**, 1444–1451.

59 M. J. Trujillo, S. L. Strausser, J. C. Becca, J. F. DeJesus, L. Jensen, D. M. Jenkins and J. P. Camden, Using SERS To Understand the Binding of N-Heterocyclic Carbenes to Gold Surfaces, *J. Phys. Chem. Lett.*, 2018, **9**, 6779–6785.

60 K. Layek, H. Maheswaran and M. L. Kantam, Ullmann coupling of aryl iodides catalyzed by gold nanoparticles stabilized on nanocrystalline magnesium oxide, *Catal. Sci. Technol.*, 2013, **3**, 1147.

61 G. Li, C. Liu, Y. Lei and R. Jin, Au25 nanocluster-catalyzed Ullmann-type homocoupling reaction of aryl iodides, *Chem. Commun.*, 2012, **48**, 12005–12007.

62 B. Karimi and F. K. Esfahani, Unexpected golden Ullmann reaction catalyzed by Au nanoparticles supported on periodic mesoporous organosilica (PMO), *Chem. Commun.*, 2011, **47**, 10452–10454.

63 K. Layek, H. Maheswaran and M. L. Kantam, Ullmann coupling of aryl iodides catalyzed by gold nanoparticles stabilized on nanocrystalline magnesium oxide, *Catal. Sci. Technol.*, 2013, **3**, 1147.

64 G. Li and R. Jin, Catalysis by gold nanoparticles: carbon-carbon coupling reactions, *Nano Rev.*, 2013, **2**, 529–545.

65 A. Monopoli, P. Cotugno, G. Palazzo, N. Ditaranto, B. Mariano, N. Cioffi, F. Ciminale and A. Nacci, Ullmann Homocoupling Catalysed by Gold Nanoparticles in Water and Ionic Liquid, *Adv. Synth. Catal.*, 2012, **354**, 2777–2788.

66 F. Khan, M. Dlugosch, X. Liu and M. G. Banwell, The Palladium-Catalyzed Ullmann Cross-Coupling Reaction: A Modern Variant on a Time-Honored Process, *Acc. Chem. Res.*, 2018, **51**, 1784–1795.

67 W. Grunert, W. Kleist and M. Muhler, *Catalysis at surfaces*, Berlin, Boston: De Gruyter, 2023.

68 G. Wang, A. Rühling, S. Amirjalayer, M. Knor, J. B. Ernst, C. Richter, H.-J. Gao, A. Timmer, H.-Y. Gao, N. L. Doltsinis, F. Glorius and H. Fuchs, Ballbot-type motion of N-heterocyclic carbenes on gold surfaces, *Nat. Chem.*, 2017, **9**, 152–156.